Received: 29 June 2022 | Revised: 23 September 2022 | Accepted: 26 September 2022

DOI: 10.1111/bph.15973

RESEARCH ARTICLE

Cannabinoid 1 (CB_1) receptor arrestin subtype-selectivity and phosphorylation dependence

Jamie J. Manning | Gabriel Rawcliffe | David B. Finlay | Michelle Glass

Department of Pharmacology and Toxicology, School of Biomedical Sciences, University of Otago, Dunedin, New Zealand

Correspondence
Michelle Glass, Department of Pharmacology and Toxicology, School of Biomedical Sciences, University of Otago, PO Box 56, Dunedin 9054, New Zealand.
Email: michelle.glass@otago.ac.nz

Funding information
Research was supported by a Health Research Council of New Zealand project grant to M. G. J. J. M. was supported by a University of Otago doctoral scholarship.

Background and purpose: Arrestin or G protein bias may be desirable for novel cannabinoid therapeutics. Arrestin-2 and arrestin-3 translocation to CB_1 receptor have been suggested to mediate different functions that may be exploited with biased ligands. Here, the requirement of a recently described phosphorylation motif '*pxxp*' (where 'p' denotes phosphorylatable serine or threonine and 'x' denotes any other amino acid) within the CB_1 receptor C-terminus for interaction with different arrestin subtypes was examined.

Experimental approach: Site-directed mutagenesis was conducted to generate nine different phosphorylation-impaired CB_1 receptor C-terminal mutants. Bioluminescence resonance energy transfer (BRET) was employed to measure arrestin-2/3 translocation and G protein dissociation of a high efficacy agonist for each mutant. Immunocytochemistry was used to quantify receptor expression.

Key results: The effects of each mutation were shared for arrestin-2 and arrestin-3 translocation to CB_1 receptor *pxxp* motifs are partially required for arrestin-2/3 translocation, but translocation was not completely inhibited until all phosphorylation sites were mutated. The *rate* of arrestin translocation was reduced with simultaneous mutation of S425 and S429. Desensitisation of G protein dissociation was inhibited in different mutants proportional to the extent of their respective loss of arrestin translocation.

Conclusions and implications: These data do not support the existence of an 'essential' *pxxp* motif for arrestin translocation to CB_1 receptor. These data also identify that arrestin-2 and arrestin-3 have equivalent phosphorylation requirements within the CB_1 receptor C-terminus, suggesting arrestin subtype-selective biased ligands may not be viable and that different regions of the C-terminus contribute differently to arrestin translocation.

KEYWORDS
arrestin, bias, cannabinoid, CB_1 receptor, GPCR, phosphorylation

Abbreviations: BRET, Bioluminescence resonance energy transfer; CTPD, C-terminal phosphorylation-deficient mutant; GIRK, G-protein-activated inward-rectifier K channels ($K_{ir}3.x$); Sp1, synthetic proline-rich peptide 1; TPD, total phosphorylation deficient mutant.

1 | INTRODUCTION

The **cannabinoid 1 (CB_1) receptor** is a G protein-coupled receptor (GPCR) which is expressed widely throughout the human brain and is involved in a range of neurological processes, such as appetite regulation, movement, learning and memory (reviewed Pacher et al., 2006). Drugs targeting CB_1 receptors therefore have potential in a range of conditions (Pacher et al., 2006), however they are limited by on-target adverse effects, such as psychoactivity and the development of tolerance.

GPCRs can activate a diverse range of different cell signalling effector pathways. 'Biased' ligands are those that selectively activate certain signalling effectors, some of which may possess clinical utility by maximising therapeutic efficacy and minimising on-target adverse events (reviewed Wootten et al., 2018). These effector subsets are commonly divided into those mediated by either the G protein or arrestin protein families, which can engage different effectors, leading to development of drugs 'biased' towards desirable effectors (Wootten et al., 2018).

CB_1 receptor activation is associated with a large range of intracellular effectors (reviewed Manning et al., 2021). Biased ligands may be valuable for the CB_1 receptor, but a key limitation for assessment of the therapeutic value of these ligands is the relatively poor characterisation of G protein versus arrestin dependent effects, and the remaining unknown requirements for arrestin interaction with CB_1 receptors.

To develop ligands biased either towards or away from arrestin proteins, an understanding of the requirements for arrestin-CB_1 receptor interaction is therefore necessary, which is the purpose of this study. It has been demonstrated that phosphorylation of a cluster of six serine/threonine residues within the extreme 'distal' CB_1 receptor C-terminus by **G protein coupled receptor kinases (GRKs)**, reviewed (Komolov & Benovic, 2018) is important for interacting with arrestin-3 (Daigle, Kwok, & Mackie, 2008) and that disrupting the ability of the C-terminus to be phosphorylated reduces receptor internalisation and enhances signalling (Daigle, Kwok, & Mackie, 2008; Hsieh et al., 1999; Jin et al., 1999; Straiker et al., 2012). In addition to this distal serine/threonine cluster, there are two serine residues near the 'proximal' end of the C-terminus (S245, S429), which have been shown via mutagenesis to be involved in receptor desensitisation, but (surprisingly) not arrestin-3 translocation (Daigle, Kearn, & Mackie, 2008; Jin et al., 1999). This 'desensitisation deficient' mutant was also suggested to have enhanced arrestin-2 interaction resulting in enhancement of pERK activation due to arrestin-2-dependent ERK scaffolding (Daigle, Kearn, & Mackie, 2008; Delgado-Peraza et al., 2016).

Despite a thorough mutagenesis study on the CB_1 receptor C-terminus (Daigle, Kwok, & Mackie, 2008), no specific phosphorylation pattern necessary for arrestin interaction with CB_1 receptor has been identified. A recent study on rhodopsin identified that a *pxxp* motif (where 'p' denotes phosphorylatable serine or threonine and 'x' denotes any other amino acid) was essential for interaction with arrestin proteins and this motif was suggested to be conserved for multiple GPCRs (Mayer et al., 2019). The 'distal' CB_1 receptor C-terminal serine/threonine cluster can form three unique *pxxp* motifs, which we hypothesised may be required for arrestin translocation and may help differentiate between the two arrestin subtypes. Additionally, the proximal S425, S429 phosphorylation sites have a known role in desensitisation and exist as a *pxxxp* motif. Given the obvious similarity of this pattern with a *pxxp* motif, we hypothesised that these sites may be similarly involved in arrestin translocation. This study therefore investigated the importance of different *pxxp* and *pxxxp* motifs on translocation of either arrestin-2 (β-arrestin-1) or arrestin-3 (β-arrestin-2) to CB_1 receptor. Additionally, to both further characterise the relationship between arrestin translocation and the desensitisation of G protein activity, and to begin to establish a functional basis for effector bias, the receptor mutants were also characterised in G protein dissociation experiments.

What is already known

- GPCR C-terminal phosphorylation is important for translocation of arrestin subtypes.
- Arrestin translocation is important for CB_1 receptor signal regulation and scaffolding functions.

What does this study add

- Identical phosphorylation sites are required for translocation of both arrestin subtypes.
- Proximal and distal phosphorylation sites are independently important for arrestin translocation.

What is the clinical significance

- These data present important considerations for development of arrestin subtype-biased ligands.

2 | METHODS

2.1 | Mutagenesis design and molecular cloning

Previously described pcDNA3 constructs containing Rluc8-(human)-Arrestin-2- synthetic proline-rich peptide 1 (Sp1) or Rluc8-(human)-arrestin-3-Sp1 (Ibsen et al., 2019) were modified for greater throughput by replacing Rluc8 (*Renilla* Luciferase) with Nluc (NanoLuc® Luciferase) via restriction cloning. The pcDNA3-Rluc8-Arrestin-2 or pcDNA3-Rluc8-Arrestin-3 vectors were amplified by PCR with primers described in Table 1 to generate

products without the Rluc8 and with specific *SfiI* sites on either end. Nluc was amplified from a GRK2-Nluc construct described previously (Matti et al., 2020), with terminal *SfiI* sites complementary to those in the arrestin fragment. Products were treated overnight at 37°C with *DpnI* to digest parental dam-methylated DNA. Products were purified using a NucleoSpin cleanup kit, then digested with *SfiI*. Products were ligated overnight at 4°C with T4 DNA ligase using 40-fmol total DNA and a vector: insert ratio of 1:3. Ligated products were purified then transformed into ultracompetent *Escherichia coli* cells (XL10 Gold). DNA was purified using QIAprep spin miniprep kits and sequence validated.

The C-terminus of human CB_1 receptor contains three possible unique *pxxp* motifs comprised of S462 and T465 (mutant D2), S464 and T467 (D3) and T465 and S468 (D4). These are substituted for alanine in the mutants denoted D2, D3 and D4 respectively (Figure 1). Because mutation of any of these sites individually leaves other functional *pxxp* motifs (e.g. mutating the sites in D2 leaves D3 as a functional *pxxp* motif), a triple mutant (S462A/S464A/T465A; T) was generated, which disrupts all *pxxp* motifs. To allow for comparison with a previous study (Daigle, Kwok, & Mackie, 2008), alanine substitution of the first (Q1) and last (Q2) four of the six serine/threonine residues was conducted (Figure 1). Additionally, all six of the serine and threonine residues in the distal C-terminus were substituted to make a C-terminal phosphorylation-deficient mutant (CTPD). A previously studied (Daigle, Kearn, & Mackie, 2008; Jin et al., 1999) 'desensitisation deficient' mutant containing two serine mutations in the proximal end of the C-terminus (S425A/S429A; D1) was also made. Finally, mutation of these proximal serine residues (D1) was performed in combination with the distal sites (CTPD) to result in a 'total phosphorylation deficient mutant' (TPD, Figure 1).

Human CB_1 receptor mutants were generated by QuikChange mutagenesis where primers were used to incorporated single or double base pair mutations into template DNA via PCR (Table 2). Products were treated overnight at 37°C with *DpnI* to digest parental dam-methylated DNA, after which the products were used to transform Aglient XL-10 gold ultracompetent *E. coli* cell, from which plasmid DNA was harvested and purified using a Qiagen miniprep kit, then sequence validated.

2.2 | Cell culture

Human Embryonic Kidney 293 cells (HEK 293; RRID:CVCL_0045) were cultured in high-glucose DMEM containing 10% ($v.v^{-1}$) FBS

TABLE 1 Cloning primers used to design the pcDNA3/Nluc-Arrestin-Sp1 constructs (forward, reverse)

Nluc fragment	AGGCCTCTGGGGCCATGGTCTTCACACTCGAAGATTTCG
	AGGCCCCGGAGGCCCCCGCCAGAATGCG
pcDNA3/Arrestin-2	AGGCCTCCGGGGCCTCCGGACTCAGATCTCGGC
	AGGCCCCAGAGGCCGGTGGCCTAGCTAGCCAG
pcDNA3/Arrestin-3	AGGCCTCCGGGGCCTCCGGACTCAGATCTCGGC
	AGGCCCCAGAGGCCGGTGGCCTAGCTAGCCAG

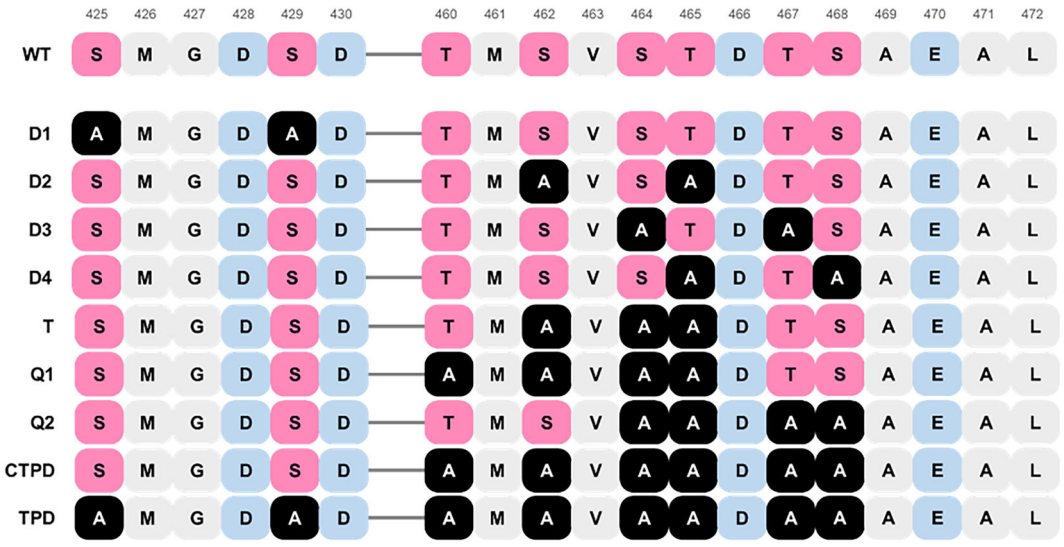

FIGURE 1 C-terminal mutants generated for this study. Serine or threonine residues were substituted to alanine in pxxxp (D1) or pxxp (D2, D3, D4) patterns. Disruption of all pxxp mutants (T) and progressive loss of the first of last four serine/threonine sites (Q1, Q2) was also conducted. Importance of proximal and distal seine/threonine residues were explored individually (D; C-terminal phosphorylation-deficient mutant 1, [CTPD]) or simultaneously (total phosphorylation deficient mutant [TPD]).

TABLE 2 Cloning primers used to design pplss-3HA-hCB$_1$ receptor mutants

CB$_1$ receptor mutation	Template CB$_1$ receptor (pEF4a)	Primer sequence (forward, reverse)
S425A/S429A	WT	CCTCTGGATAACGCCATGGGGGACGCGGACTGCCTGC
		GCAGGCAGTCCGCGTCCCCCATGGCGTTATCCAGAGG
S464A	WT	GGTAACCATGTCTGTGGCCACAGACACGTCTGC
		GCAGACGTGTCTGTGGCCACAGACATGGTTACC
T465A	WT	CATGTCTGTGTCCGCAGACACGTCTGCC
		GGCAGACGTGTCTGCGGACACAGACATG
T467A	WT	GTGTCCACAGACGCGTCTGCCGAGGCTC
		GAGCCTCGGCAGACGCGTCTGTGGACAC
S468A	WT	GTCCACAGACACGGCTGCCGAGGCTC
		GAGCCTCGGCAGCCGTGTCTGTGGAC
S462A/T465A	T465A	GCCAAGGTAACCATGGCTGTGTCCGCAGACA
		TGTCTGCGGACACAGCCATGGTTACCTTGGC
S464A/T467A	WT	ACCATGTCTGTGGCCACAGACGCGTCTGCCGAGG
		CCTCGGCAGACGCGTCTGTGGCCACAGACATGGT
T465A/T468A	T465A	GTCCGCAGACACGGCTGCCGAGGCTC
		GAGCCTCGGCAGCCGTGTCTGCGGAC
S462A/S464A/T465A	S462A/T465A	GTAACCATGGCTGTGGCCGCAGACACGTCTG
		CAGACGTGTCTGCGGCCACAGCCATGGTTAC
T460A/S462A/S464A/T465A	S462A/S464A/T465A	TCAAGATTGCCAAGGTAGCCATGGCTGTGGCC
		GGCCACAGCCATGGCTACCTTGGCAATCTTGA
S464A/T465A/T467A/S468A	T456A/S468A	CCATGTCTGTGGCCGCAGACGCGGCTGCCGAG
		CTCGGCAGCCGCGTCTGCGGCCACAGACATGG
T460A/S462A/S464A/T465A/T467A/S468A	T460A/S462A/S464A/T465A	GTCAAGATTGCCAAGGTAGCCATGGCTGTGGCCGCA
		TGCGGCCACAGCCATGGCTACCTTGGCAATCTTGAC

and grown in an incubator at 37°C in a humidified atmosphere containing 5% CO_2. Cells were grown in vented-cap 75-cm^2 cell culture flasks and were sub-cultured using 0.05% trypsin-EDTA when approximately 80% confluency was achieved.

2.3 | Bioluminescence resonance energy transfer (BRET) assays

HEK293 cells were passaged and seeded into wells of a 6-well culture plate at a density which resulted in 30%–40% confluence within 24–48 h of growth. Medium was replaced and cells were transfected as below.

The transfection protocol for **arrestin translocation** to unmodified receptors (Donthamsetti et al., 2015) employed here is based on a previously described 100 mm culture dish protocol for CB$_1$ receptor using 4 μg total DNA (Finlay et al., 2019; Ibsen et al., 2019), with all transfection reagents scaled down by surface area (∼1/5.79) for use in six-well cell culture plates. A mixture of 690 ng total DNA consisting of plasmids encoding the membrane-tethered BRET acceptor citrine (pcDNA3/mem-linker-citrine-Src Homology domain of *Saccharomyces cerevisiae* Sho1 [SH3], 345 ng), the Nluc-conjugated arrestin-2/3 BRET donor (pcDNA3, 9 ng, molar ratio of 1:40 donor: acceptor), triply-haemagglutinated receptor expressed at high levels via the pre-prolactin signal sequence (pEF4a/pplss-3HA-hCB$_1$ receptor; Wild type or mutant variants, 276 ng) and empty pcDNA3.1+ (60 ng) was incubated for 20 min at room temperature with 6 μg PEI Max (1:9 DNA:PEI) in a total volume of 200 μl OptiMEM.

For **G protein dissociation** BRET transfection, a single pIRES vector containing genes encoding Nluc-Gαi_3 and G$\beta_1\gamma_2$-cpVenus was used, as described previously (Matti et al., 2020; Patel et al., 2022). This vector (777 ng) was mixed with pplss-3HA-hCB$_1$ receptor constructs (pEF4a, 276 ng) and 60 ng empty vector (pcDNA3) in 200-μl OptiMEM with 10 μg PEI Max (1:9 DNA:PEI) and incubated for 20 min at room temperature.

Transfection mixtures were gently added dropwise to wells and cultured overnight. Transfected cells were lifted with typsin and seeded into poly-d-lysine-coated (0.05 mg·ml^{-1}, 30 min) white 96-well CulturPlates at a density of 4 × 10^4 cells per well and were grown overnight. In parallel, cells were seeded into clear plastic 96-well plates for immunocytochemical analysis (below).

Cells were serum starved in 'assay medium', composed of phenol-red free high glucose DMEM and 25 mM HEPES,

supplemented with 1 mg·ml^{-1} BSA for 30 min, after which they were treated with 5 μM coelenterazine-h. Donor and acceptor wavelengths of 475 and 535 nm were simultaneously detected every 25–37 s at 37°C in a LumiSTAR (BMG Labtech, Ortenberg, BW, Germany) following coelenterazine addition for 5 min to establish a baseline. Serial dilutions of MDMB-Fubinaca were subsequently added such that final well volume was 100 μl, and responses were measured for 25 min.

2.4 | Immunocytochemistry

Transfected cells from the BRET assays were plated into clear plastic 96-well plates at a density of 4×10^4 cells per well (as above) and grown overnight. Growth medium was removed and live cells were incubated with mouse monoclonal anti-HA.11 IgG (clone 16B12, RRID:AB_2565005) diluted 1/500 in assay medium for 30 min at room temperature to label **cell surface** receptors only. Primary antibody was aspirated and cells were twice washed with phosphate buffered saline (PBS), then fixed in 4% (w·v^{-1}) paraformaldehyde in 0.1-M PBS for 15 min at room temperature. Paraformaldehyde was aspirated and cells were washed with PBS. To label **total receptor**, cells were first fixed, then labelled with 1/1000 mouse monoclonal anti-HA.11 IgG either at room temperature (rocking) for 3 h, or overnight at 4°C. Primary antibody was labelled with secondary antibody, Alexa Fluor® 594 goat anti-mouse IgG (RRID:AB_2534091) diluted in immunobuffer (PBS supplemented with 1% goat serum, 0.2% Triton X-100 and 0.4-mg·ml^{-1} merthiolate) at a dilution of 1/500 at either room temperature on a plate shaker for 3 h, or 4°C overnight. Antibody was removed and cells were twice washed with PBS, then nuclei were stained by incubation with 8 ng·ml^{-1} Hoechst 33258 in MilliQ H_2O for 15 min at room temperature. Finally, Hoechst was removed and cells were twice washed with PBS-T then stored in PBS-T containing 0.4 mg·ml^{-1} merthiolate.

Plates were imaged on an Opera Phenix® Plus microscope (PerkinElmer). Acquisitions used 20X objective magnification, and excitation/emission settings were 375/430–480 nm (~20 ms, for Hoechst detection), and 561/570–630 nm (~1000 ms, for AlexaFluor® 594). Images were analysed in Columbus (version 2.9.1). Raw images were analysed for total grey area per cell, by adapting analysis journals previously described for another high content system into Columbus software (Finlay et al., 2016; Grimsey et al., 2008). In brief, cells were located and counted using the 'Find Nuclei' tool. A receptor staining mask (Alexa 594 fluorescence) was then applied to define a region for analysis in the 561 nm channel ('Image Region'). This region was then quantified for absolute threshold intensity (above a user-defined 'background'), and this value was divided by the number of nuclei counted in the 375 nm channel. Results from 25 imaged sites/well were then averaged; these means were used for each well. The Immuno-related procedures used comply with the recommendations made by the *British Journal of Pharmacology* (Alexander et al., 2018).

2.5 | Kinetic analyses

Raw BRET ratios were baseline-corrected by subtracting the time course of the vehicle-treated condition of each stimulation (ΔBRET ratio). These data were modelled by previously described kinetic equations (Hoare et al., 2020, 2022). Arrestin translocation data were modelled by the 'rise to steady state' equation, which quantifies translocation steady state, translocation half-time, and approximates the initial rate of signal generation. Baseline was constrained as zero, as the data had been corrected to matched vehicle conditions.

Similarly, G protein dissociation data were modelled by the 'fall-rise to baseline' equation, also described previously (Hoare et al., 2020). Baseline was constrained to zero, and k2 (desensitisation rate constant) was constrained to >0.0001 (desensitisation half-time of less than 6931 s).

Area under curve (AUC) was also determined in Graphpad Prism (version 9.4.0., GraphPad Software LLC, San Diego, CA, USA) to report net changes in BRET over the entire time course.

2.6 | Data and statistical analysis

Where possible, all mutant receptors were tested together with a wild type control in each experiment, with $n = 5$ for each mutant in order to allow for statistical analysis according to the *British Journal of Pharmacology* guidelines (Curtis et al., 2022). In these experiments, mutants were compared to wild type using a randomised block ANOVA followed by Dunnett's multiple comparisons test conducted in GraphPad Prism. In some instances, due to scale, it was not feasible to include all mutants in the same experiment. To ensure $n = 5$ for each mutant, more data for the matched wild type receptor had to be generated, resulting in a greater n for wild type. These datasets were analysed using a mixed-effects randomised block analysis followed by Dunnett's multiple comparisons test. In all cases, statistical analysis was performed on non-normalised data, which in some instances was then reported as a mean normalised to each matched wild type response. As all assays were performed in 96-well plates, blinding was unfeasible for all experimental and data analysis procedures. A significance level of 0.05 was used throughout this study, and post hoc tests were only conducted if the F statistic in ANOVA achieved this level of significance. In some cases, parameters were unable to be defined due to the absence of a response. In these cases, the effect size is denoted as not determined (n/d).

2.7 | Materials

2.7.1 | Molecular biology materials

Primers were purchased from Integrated DNA Technologies (Coralville, Iowa, USA). All restriction enzymes were purchased from New England Biolabs (Ipswich MA, USA). Nucleospin PCR cleanup kits

were purchased from Macherey-Nagel (Düren, NRW, Germany). T4 DNA Ligase was purchased from Promega (Madison, WI, USA). Ultra-competent XL-10 Gold *E. coli* were purchased from Agilent technologies (Santa Clara, CA, USA). QIAprep spin miniprep kits were purchased from Qiagen (Hilden, NRW, Germany).

2.7.2 | Cell culture, transfection, and BRET materials

High-glucose DMEM (± phenol-red), trypsin-EDTA, and OptiMEM, were purchased from Thermo Fisher Scientific (Waltham, MA, USA). PEI Max was sourced from Polysciences (Warrington, MA, U.S.A.). NZ-origin FBS was purchased from Moregate Biotech (Brisbane, Australia). BSA was sourced from MP Biomedicals (Auckland, New Zealand). Vented-cap 75 cm^2 culture flasks were from Corning (Corning, NY, USA), and 6-well plates; were from Greiner Bio-One GmbH (Kremsmünster, Austria). Poly-D-Lysine was purchased from Sigma-Aldrich (St. Louis, MO, USA). White 96-well CulturPlates were from PerkinElmer (Waltham, MA, USA). Coelenterazine-h was sourced from Nanolight Technology (Pinetop, AZ, USA).

2.7.3 | Immunocytochemical materials

Mouse monoclonal anti-HA.11 IgG was purchased by BioLegend (Cat# 901503; San Diego, CA, USA). Alexa Fluor® 594 goat anti-mouse IgG; Thermo Fisher Scientific (Cat# A11032). Clear-plastic 96-well plates from Corning. Triton X-100, paraformaldehyde, Hoechst33258, and Merthiolate were purchased from Sigma-Aldrich. Goat serum was from Thermo Fisher Scientific. MDMB-Fubinaca was purchased from Cayman Chemical Co (Ann Arbor, MI, USA).

2.8 | Nomenclature of targets and ligands

Key protein targets and ligands in this article are hyperlinked to corresponding entries in the IUPHAR/BPS Guide to PHARMACOLOGY http://www.guidetopharmacology.org and are permanently archived in the Concise Guide to PHARMACOLOGY 2021/22 (Alexander et al., 2021).

3 | RESULTS

3.1 | Translocation of arrestin-2 to CB_1 receptor mutants

MDMB-Fubinaca is a highly efficacious synthetic cannabinoid receptor agonist, which activates CB_1 receptor with high potency (Banister et al., 2016; Gamage et al., 2018) and has been demonstrated via cryo-electron microscopy to stabilise an active receptor state (Krishna Kumar et al., 2019). It is an L-*tert*-leucinate analogue of the L-valinate indazole-3-carboxamide AMB-Fubinaca, sharing the high efficacy attributes of this ligand, including in the arrestin translocation pathway previously characterised, making it an effective candidate ligand for probing loss of arrestin translocation (Finlay et al., 2019; Sachdev et al., 2019).

Translocation of arrestin-2 to wild type CB_1 receptor occurred following stimulation with MDMB-Fubinaca (100 nM). The kinetic

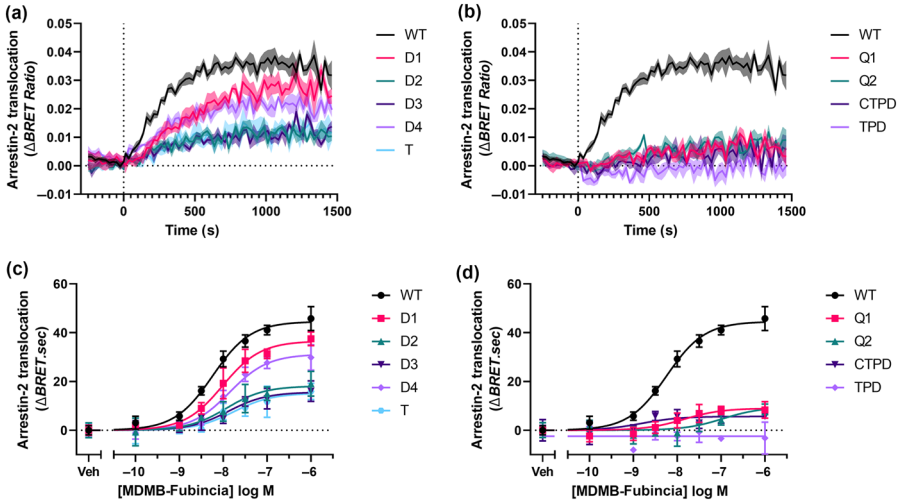

FIGURE 2 Ability of different CB_1 receptor C-terminal receptor mutants to facilitate arrestin-2 translocation. HEK293 cells transiently expressing pplss-3HA-tagged CB_1 receptor (WT or mutants) and arrestin-2 translocation BRET assay components were stimulated with MDMB-Fubinaca (100 nM) for 25 min. Time series BRET data of the kinetic response for each mutant are depicted in (a) and (b), where lines represent mean ΔBRET ratio and shading represents SEM of five experimental repeats (each conducted in triplicate). AUC was calculated to determine net translocation for concentration-responses depicted in (c) and (d), where each data point is the mean and associated SD, fit with a three-parameter sigmoidal curve for a single representative experiment conducted in technical triplicate and repeated five times.

profile of arrestin-2 translocation showed an initial rapid recruitment following stimulation, followed by a steady state that was maintained for the remaining recording period. This time course was modelled with a 'rise to steady state' equation to measure initial translocation rate, translocation half time and steady state of translocation for saturating concentration of ligand, as recommended (Hoare et al., 2020). Importantly, each of these parameters represents efficacy in distinct ways: increasing efficacy corresponds to more rapid rates and smaller half times of translocation, which may or may not *also* manifest in an increased steady state of translocation (described below). This study has also investigated translocation efficacy using net translocation over the recording period (AUC) in order to obtain the classical pharmacological parameters E_{Max} and pC_{50}.

Wild type CB_1 receptor stimulated with MDMB-Fubinaca (100 nM) elicited arrestin-2 translocation with a half-time of 185 s, reaching a steady state of 0.036 ΔBRET ratio units (Figure 2 and Table 3). The three different *pxxp* mutants in the distal C-terminus (D2, D3, and D4) exhibited partially reduced translocation steady states, but no significant change in half time (Figure 2 and Table 3), as did a mutant lacking any *pxxp* motifs (T). In comparison, mutants with ≥4 mutations to the C-terminus (Q1, Q2, CTPD and TPD) did not elicit measurable translocation of arrestin-2 (Figure 2 and Table 3). Comparatively, the 'desensitisation deficient' *pxxxp* mutant (D1, S425A/S429A) did *not* exhibit a reduced translocation steady state, but did exhibit reduced translocation half time, taking longer to reach 'maximum' translocation steady state (Figure 2 and Table 3). The initial rate of translocation has been suggested as a useful efficacy metric as it approximates signalling efficacy at $t = 0$, prior to any negative feedback (Hoare et al., 2020). Indeed, despite different kinetic profiles reported above, the initial rate of arrestin-2 translocation to CB_1 receptor was reduced in all mutants, capturing changes in both half time and steady state (Table 3).

Net arrestin-2 translocation over 25 min occurred with a potency of 6 nM for the wild type receptor, with no changes in any of the mutants (Figure 2 and Table 4). Net efficacy of each mutant was reduced compared to wild type in line with the reported reductions to steady state, except for the D1 mutant of CB_1 receptor, which had reduced net arrestin-2 translocation (despite equivalent steady state) as a result of the slower association kinetics (Figure 2 and Table 4).

3.2 | Translocation of arrestin-3 to CB_1 receptor mutants

All C-terminal phosphorylation mutants were also examined for their ability to elicit arrestin-3 translocation to determine whether different phosphorylation motifs are implicated for translocation of the two arrestin subtypes. As previously reported (Ibsen et al., 2019), arrestin-3 translocation was of greater magnitude than arrestin-2, with wild type CB_1 receptor reaching a mean translocation steady state of 0.125 ΔBRET units (Figure 3 and Table 3) in response to MDMB-Fubinaca (100 nM). Additionally, arrestin-3 translocation to wild type CB_1 receptor occurred more rapidly than arrestin-2, with a mean translocation half time of 85.6 s (Figure 3 and Table 3).

The consequences of CB_1 receptor C-terminal mutation on translocation of arrestin-3 were similar to those for arrestin-2. The *pxxxp* mutant D1 reached the same steady state as wild type CB_1 receptor with a significantly slower translocation half time and the D2 *pxxp* mutant had a slightly faster half time (Figure 3 and Table 3). Two of

TABLE 3 Kinetic parameters of arrestin-2 and arrestin-3 translocation of MDMB-Fubinaca (100 nM)

	Arrestin-2							Arrestin-3						
	Steady state (ΔBRET ratio)		Translocation half time (s)		Initial rate (1×10^6 ΔBRET ratio per second)			Steady state (ΔBRET ratio)		Translocation half time (s)		Initial rate (1×10^6 ΔBRET ratio per second)		
	Mean	SEM	Mean	SEM	Mean	SEM	n	Mean	SEM	Mean	SEM	Mean	SEM	n
WT	0.036	0.002	185.0	8.3	136.1	5.5	5	0.125	0.005	85.6	2.8	1027.0	49.5	15
D1	0.036	0.004	569.2[a]	181.4	58.1[a]	11.4	5	0.115	0.004	163.5[a]	5.8	491.4[a]	32.8	5
D2	0.012[a]	0.001	285.8	82.6	37.7[a]	8.2	5	0.063[a]	0.005	60.3[a]	5.7	742.9[a]	84.3	5
D3	0.014[a]	0.002	354.0	103.1	30.6[a]	3.4	5	0.069[a]	0.004	98.9	4.3	486.3[a]	22.1	5
D4	0.022[a]	0.002	210.5	16.3	73.1[a]	6.6	5	0.106	0.015	96.5	10.1	768.1[a]	87.3	5
T	0.014[a]	0.003	353.6	73.2	33.2[a]	11.0	5	0.056[a]	0.005	88.7	8.1	437.6[a]	19.4	5
Q1	n/d	-	n/d	-	n/d	-	5	0.044[a]	0.004	95.8	9.3	345.0[a]	65.5	5
Q2	n/d	-	n/d	-	n/d	-	5	0.038[a]	0.002	83.7	6.1	315.5[a]	25.4	5
CTPD	n/d	-	n/d	-	n/d	-	5	0.027[a]	0.003	76.7	9.3	264.0[a]	49.5	5
TPD	n/d	-	n/d	-	n/d	-	5	0.011[a]	0.003	n/d	-	n/d	-	5

Abbreviations: BRET, Bioluminescence resonance energy transfer; CTPD, C-terminal phosphorylation-deficient mutant; TPD, total phosphorylation deficient mutant.

[a]Statistically significant difference compared to experimentally matched WT CB_1 receptor using randomised block two-way ANOVA followed by Dunnett's post hoc multiple comparisons test.

TABLE 4 Concentration-response parameters of net arrestin-2/3 translocation of CB_1 receptor WT and each mutant in response to MDMB-Fubinaca stimulation for 25 min. E_{Max} values are normalised to the experimentally-matched hCB_1 receptor WT response

	Arrestin-2					Arrestin-3				
	Emax (%WT)		pC_{50} (−log M)			Emax (%WT)		pC_{50} (−log M)		
	Mean	SEM	Mean	SEM	n	Mean	SEM	Mean	SEM	n
WT	100.0	0.0	8.19	0.10	5	100.0	0.0	8.42	0.03	15
D1	72.3[a]	6.3	8.06	0.06	5	77.4[a]	1.0	8.03	0.07	5
D2	32.3[a]	3.8	7.73	0.10	5	47.7[a]	3.2	8.52	0.04	5
D3	32.9[a]	2.6	8.20	0.26	5	57.6[a]	5.3	8.34	0.06	5
D4	61.6[a]	6.6	8.02	0.08	5	86.5	12.2	8.26	0.03	5
T	25.6[a]	3.4	8.14	0.25	5	44.4[a]	4.8	8.38	0.05	5
Q1	14.1[a]	3.0	8.23	0.31	5	39.0[a]	6.7	8.33	0.05	5
Q2	20.9[a]	2.0	8.22	0.40	5	33.3[a]	2.6	8.47	0.07	5
CTPD	n/d	n/d	n/d	n/d	5	25.9[a]	2.2	8.39	0.13	5
TPD	n/d	n/d	n/d	n/d	5	9.6[a]	0.9	8.63	0.41	5

Abbreviations: CTPD, C-terminal phosphorylation-deficient mutant; TPD, total phosphorylation deficient mutant.
[a]Statistically significant difference compared to experimentally-matched non-normalised WT CB_1 response using repeated measures two-way ANOVA followed by Dunnett's post hoc multiple comparisons test.

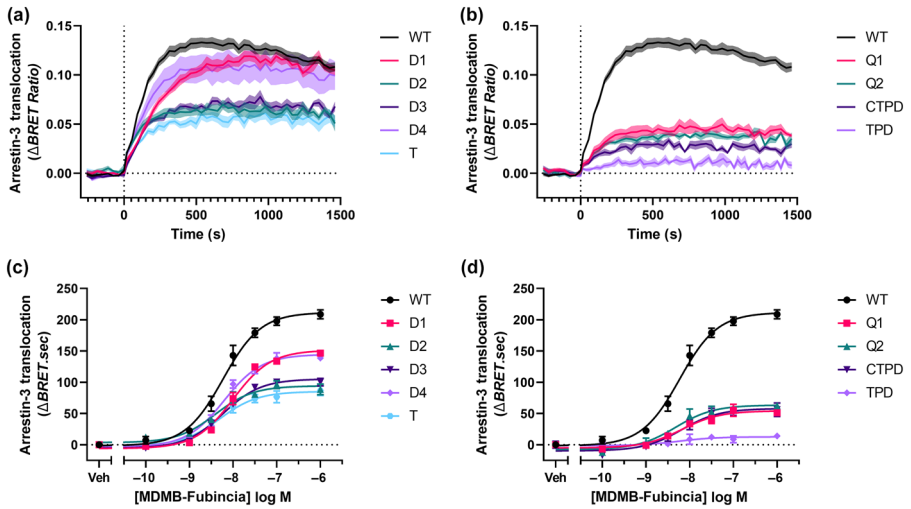

FIGURE 3 Arrestin-3 translocation to different CB_1 receptor C-terminal receptor mutants. HEK293 cells transiently expressing pplss-3HA-hCB_1 receptor WT or mutants and arrestin translocation BRET assay components were stimulated for 25 min with 100 nM MDMB-Fubinaca. Kinetic time series data are shown for each mutant in (a) and (b), where lines represent mean ΔBRET ratio and shading represents the associated SEM (n = 15, WT; n = 5, each mutant). (c,d) AUC-derived concentration-response data of each mutant, showing mean ΔBRET.sec and associated SD of a representative experiment conducted in triplicate and repeated five times for each mutant.

the three *pxxp* mutants D2 and D3 exhibited partially reduced translocation steady state with the same half time as wild type CB_1 receptor following stimulation with 100-nM MDMB-Fubinaca (Figure 3 and Table 3). The mutant in which all *pxxp* motifs were disrupted (T) also demonstrated partial reduction of arrestin-3 translocation by MDMB-Fubinaca (100 nM), similar to the D2 and D3 mutants (Figure 3 and Table 3). Mutation to the first (Q1) or last (Q2) four serine threonine sites in the distal C-terminus further reduced translocation steady state, as did mutation of all phosphorylation sites in the distal C-terminus (CTPD; Figure 3 and Table 3). However, simultaneous mutation of the *pxxxp* motif within the proximal C-terminus and all of the phosphorylation sites within the distal C-terminus (TPD) completely attenuated the ability of CB_1 receptor to interact with arrestin-3 following activation with MDMB-Fubinaca (100 nM; Figure 3 and Table 3). Consistent with reductions to either translocation half time or steady states, all mutants had significantly reduced initial translocation rates, including the D1 mutant, which had a reduced activation half time.

Analogous to arrestin-2, changes in net arrestin-3 translocation were comparable to changes in steady state for most mutants, except for D1 where the reduction in rate was associated with reduced net translocation (Figure 3 and Table 4). No changes in the potency of

MDMB-Fubinaca-mediated arrestin-3 translocation were observed for any of the mutants (where measurable; Figure 3 and Table 4).

3.3 | Changes in G protein dissociation of CB_1 receptor C-terminal mutants

The effects of reduced arrestin interaction on the ability of CB_1 receptor to cause G protein dissociation and desensitisation were directly measured by BRET using a reporter described previously (Matti et al., 2020; Patel et al., 2022) and modelled using a 'baseline followed by fall-rise to baseline' equation (Hoare et al., 2020). Wild type CB_1 receptor caused rapid (half time 16.7 sec; Table 5) dissociation of $G\alpha_{i3}$ from $G\beta_1\gamma_2$ in response to stimulation with MDMB-Fubinaca (100 nM), which reached a mean peak dissociation of 0.100 ΔBRET units (Figure 4, Table 5). Following peak dissociation levels, the response slowly desensitised, with an estimated mean half time of 1,217 seconds (~20 min; Figure 4 and Table 5).

All of the C-terminal mutants displayed dramatically altered profiles of G protein dissociation in response to MDMB-Fubinaca

TABLE 5 Kinetic parameters of G protein dissociation following stimulation of CB_1 receptor mutants with 100 nM MDMB-Fubinaca

	Peak (ΔBRET ratio)		Activation half time (s)		Desensitisation half time (s)		Initial rate (1×10^{-3} ΔBRET ratio per second)		
	Mean	SEM	Mean	SEM	Mean	SEM	Mean	SEM	n
WT	−0.100	0.008	16.9	1.9	1,219	226.3	4.99	0.74	9
D1	−0.184[a]	0.010	18.3	3.6	1711	210.7	8.99[a]	2.28	5
D2	−0.155[a]	0.002	28.5[a]	4.5	3348[a]	548.2	4.39	0.76	5
D3	−0.153[a]	0.010	22.9	2.7	4170[a]	812.3	5.00	0.56	5
D4	−0.163[a]	0.006	23.0	2.6	2648[a]	414.1	5.44	0.70	5
T	−0.164[a]	0.006	21.1	1.1	5910[a]	540.4	5.59	0.37	5
Q1	−0.158[a]	0.011	34.5[a]	4.7	>6931	-	3.59	0.68	5
Q2	−0.169[a]	0.011	20.5	1.5	>6931	-	5.96	0.64	5
CTPD	−0.163[a]	0.010	31.6[a]	4.6	>6931	-	4.04	0.68	5
TPD	−0.169[a]	0.012	28.9[a]	3.6	>6931	-	4.55	0.82	5

Abbreviations: BRET, bioluminescence resonance energy transfer; CTPD, C-terminal phosphorylation-deficient mutant; TPD, total phosphorylation deficient mutant.

[a]Statistically significant difference compared to experimentally-matched WT CB_1 receptor response using randomised block two-way ANOVA followed by Dunnett's post hoc multiple comparisons test.

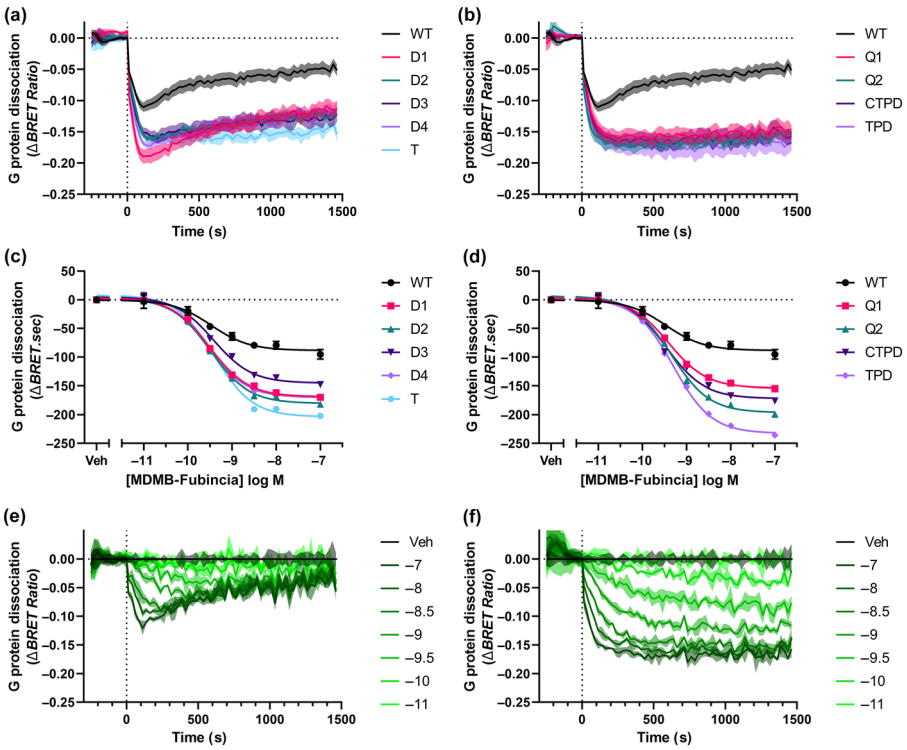

FIGURE 4 G protein activity of CB_1 receptor C-terminal mutants. HEK293 cells were transfected with pplss-3HA-tagged CB_1 receptor WT or mutants, arrestin-3 and a BRET-based G protein dissociation reporter and were stimulated with 100 nM MDMB-Fubinaca for 25 min. The responses elicited by each mutant are shown (a, b), where lines are mean ΔBRET ratio and shading is the associated SEM (n = 9, WT, n = 5, each mutant). AUC-derived concentration-response curves for each mutant are depicted in (c) and (d), where data are mean and SD of triplicates from a representative experiment. Dilution series of MDMB-Fubinaca for a representative experiment in triplicate are displayed for WT CB_1 receptor (e) and total phosphorylation deficient mutant (TPD) CB_1 receptor mutant (f).

(100 nM) compared to the wild type receptor. The proximal *pxxxp* mutant (D1) elicited a considerably enhanced peak dissociation (84% greater than wild type; Table 5) and a modestly (but not significantly) slower desensitisation half time. The three individual *pxxp* mutants, and the triple mutant with no *pxxp* motifs, all of which displayed partially reduced arrestin-2 and arrestin-3 translocation, exhibited an approximate 50% increase in peak G protein dissociation, with desensitisation half times slowed between two- (D4) and five-fold (T). The larger-scale reductions to arrestin-2 and arrestin-3 translocation in the Q1, Q2, CTPD and TPD mutants were associated with significantly enhanced peak dissociation (~60% greater than wild type; Table 5). In addition to enhanced peak dissociation, there was a complete abrogation of desensitisation; for these four mutants, desensitisation half-life was unable to be estimated, as they were significantly greater than the constraint of 6931 s (k2; Table 5). This loss of desensitisation was (qualitatively) preserved at all concentrations of agonist, as shown for the TPD mutant of CB_1 receptor compared to the wild type (Figure 4).

All of the C-terminal mutants studied exhibited significantly enhanced G protein dissociation E_{Max} values, consistent with the observed changes in kinetics (Figure 4 and Table 6). Additionally, all mutants displayed reduced G protein dissociation potency, albeit with mean differences of less than 0.31 nM (Figure 4 and Table 6).

TABLE 6 Concentration-response parameters of G protein dissociation of CB_1 receptor C-terminal mutants by MDMB-Fubinaca

	pC50 (−log M)		Dissociation E_{Max} (ΔBRET.sec)		
	Mean	SEM	Mean	SEM	n
WT	9.66	0.04	−99.7	12.9	9
D1	9.42[a]	0.07	−218.0[a]	15.0	5
D2	9.45[a]	0.02	−196.9[a]	4.8	5
D3	9.39[a]	0.04	−197.2[a]	15.2	5
D4	9.45[a]	0.04	−201.6[a]	9.6	5
T	9.34[a]	0.04	−225.6[a]	8.9	5
Q1	9.36[a]	0.02	−218.6[a]	16.7	5
Q2	9.28[a]	0.02	−236.8[a]	12.9	5
CTPD	9.37[a]	0.05	−226.7[a]	15.3	5
TPD	9.30[a]	0.03	−249.9[a]	12.1	5

Abbreviations: BRET, bioluminescence resonance energy transfer; CTPD, C-terminal phosphorylation-deficient mutant; TPD, total phosphorylation deficient mutant.
[a]Statistical significance compared to WT using repeated measures one-way ANOVA followed by Dunnett's multiple comparisons test.

3.4 | Receptor expression of mutants in different BRET assays

To rule out the possibility of altered pharmacological responses for each mutant being attributed to changed receptor expression in the above BRET assays, cells from each assay were immunolabelled to evaluate whether the mutants exhibited differing expression levels. Some variation between mutants was detected (~ ±35%), though not reaching significance for the cell surface expression (live immunolabelling) of receptor in the G protein dissociation experiments (Table 7). The only significant differences for the arrestin-2 assays were higher surface expression (live immunolabelling) of D1 and D4 (Table 7), which may mean losses of arrestin-2 translocation for these mutants are understated. Comparatively, total (post-fixation) receptor expression of CTPD and TPD were significantly reduced in the arrestin-3 assays. Whilst cell-surface receptor expression was measured only for n = 2 replicates for all mutants except for D1 and TPD in the

TABLE 7 Receptor expression of each CB_1 receptor C-terminal mutant in each assay employed in this study. Data are total grey level per cell normalised to each experimentally-matched wild type receptor.

	Surface expression									Total expression		
	G protein dissociation			Arrestin-2 translocation			Arrestin-3 translocation			Arrestin-3 translocation		
	Mean	SEM	n	Mean	SEM	n	Mean	SEM	n	Mean	SEM	n
WT	100.0	0.0	9	100	0.0	5	100.0	0.0	10	100.0	0.0	15
D1	183.3	40.2	5	159.8[a]	9.3	5	84.1	32.4	5	117.8	12.8	5
D2	99.9	6.2	5	126.0	9.2	5	74.5	16.8	2	89.2	12.7	5
D3	95.0	5.4	5	142.2	3.4	5	89.7	40.6	2	110.5	17.0	5
D4	152.9	32.8	5	181.7[a]	25.9	5	148.8	69.1	2	144.3	32.7	5
T	104.2	6.0	5	119.2	6.0	5	93.2	49.5	2	92.8	19.1	5
Q1	81.9	4.5	5	96.8	10.7	5	66.1	24.2	2	84.5	15.4	5
Q2	101.3	6.1	5	125.1	16.0	5	68.7	22.7	2	69.4	8.3	5
CTPD	91.0	4.6	5	94.9	7.6	5	57.4	29.8	2	57.7[a]	12.6	5
TPD	104.3	5.0	5	78.1	7.7	5	88.2	1.3	5	84.2[a]	3.7	5

Abbreviations: CTPD, C-terminal phosphorylation-deficient mutant; TPD, total phosphorylation deficient mutant.
[a]Statistical significance compared to WT using repeated measures one-way ANOVA followed by Dunnett's multiple comparisons test.

arrestin-3 experiments (which were not significantly different to wild type), these appear to be accurately reflected by total expression measurements, and an absence of large differences in expression may therefore be inferred (Table 7).

4 | DISCUSSIONS AND CONCLUSIONS

4.1 | *pxxp* motifs are not essential and are not arrestin subtype-specific

This study identifies several important elements of the translocation of arrestin-2 and arrestin-3 to human CB_1 receptor, and the consequences of arrestin recruitment on G protein dissociation. A core aim of this study was to investigate whether any of the three possible *pxxp* motifs within the C-terminus of CB_1 receptor were necessary for interaction with either arrestin-2 or arrestin-3. This aim was based on the observation in a previous study that a *pxxp* motif was essential for interaction between the two arrestins and the rhodopsin receptor, and the suggestion that such a motif is important for many **family A (rhodopsin-like family) GPCRs** (Mayer et al., 2019). The data presented in this study do not support this hypothesis for CB_1 receptors; no single *pxxp* motif was 'essential' to translocation of either arrestin-2 or arrestin-3 to CB_1 receptor, although perturbation of any of the three motifs conferred ~50% loss in arrestin translocation. This may suggest that individual *pxxp* mutation leaves other adjacent *pxxp* motifs that can still bind arrestin-2 or arrestin-3. However, a mutant that disturbed all pxxp sites (but still maintained some phosphorylatable sites in the region) also exhibited approximately 50% loss, suggesting that the motifs themselves are not critical. This observation is congruent with earlier studies on the phosphorylation sites within the rat CB_1 receptor C-terminus. Previous alanine substitution of adjacent pairs of serine/threonine residues (rCB_1 receptor notation: T461/S463, S465/T466, T468/S469, equivalent to human notation: T460/S462, S464/T465, T467/S468) resulted in no significant change to arrestin-3 translocation (Daigle, Kwok, & Mackie, 2008).

Importantly, this study identifies that arrestin-2 and arrestin-3 translocation to CB_1 receptor in response to MDMB-Fubinaca are similarly perturbed in response to each alanine substitution, suggesting that these two arrestin subtypes require interaction with the same phosphorylated sites. Taken together with previously-reported data showing that several cannabinoid ligands facilitate arrestin-2/3 translocation to CB_1 receptor in a relatively unbiased manner (i.e. arrestin-2 efficacy is proportional to arrestin-3 efficacy; Finlay et al., 2019; Patel et al., 2020), it therefore seems that the extent of receptor phosphorylation is efficacy-dependent and drives translocation of both arrestin subtypes. This observation suggests that selective interaction with individual arrestin subtype is not possible based on phosphorylation pattern alone, as arrestin-2 and arrestin-3 translocation appear to be inextricable. Therefore, developing arrestin subtype-biased ligands on the basis of different phosphorylation patterns may not be possible. Lower efficacy ligands such as **Δ^9-THC** or **anandamide** however, may display different sensitivity to each mutant based on this possible efficacy-dependence of phosphorylation.

4.2 | Reduced arrestin translocation produces potentiated signalling

Whilst this study, along with those previous, does not identify an essential motif for arrestin-2/3 translocation, the importance of the distal cluster of serine/threonine residues in translocation and subsequent receptor activity are validated. This 'distal cluster' has previously been reported to be involved in both arrestin translocation (Daigle, Kwok, & Mackie, 2008) and internalisation (Daigle, Kwok, & Mackie, 2008; Hsieh et al., 1999; Jin et al., 1999). Additionally, mutation or truncation of this distal cluster has been observed to significantly potentiate CB_1 receptor pERK signalling (Daigle, Kearn, & Mackie, 2008), postsynaptic current inhibition (Straiker et al., 2012), but not **GIRK (K_{ir})** channel activation (Jin et al., 1999). This study identifies that peak G protein activity is very sensitive to loss of arrestin translocation, as most mutants conferred a doubling of G protein activity. Additionally, reduced arrestin translocation was associated with reduced desensitisation of G protein dissociation, meaning that loss of arrestin-2/3 translocation potentiates G protein signalling by abolishing arrestin-mediated negative feedback. This appears incongruent with CB_1 receptor-arrestin co-localisation data reported in a previous study, where three double mutants had unchanged arrestin interaction but potentiated pERK signalling (Daigle, Kwok, & Mackie, 2008). Given that in HEK293 cells, the pERK signal is predominantly G protein mediated (Finlay et al., 2017), it is likely that these mutants had greater pERK signalling due to partial loss of arrestin translocation that the immunocytochemical method previously may not have been sufficiently sensitive to detect. The former study also investigated the rat isoforms of the Q1 and CTPD mutants employed in this study, reporting that neither could cause arrestin translocation or CB_1 receptor internalisation, in close agreement with the results reported here (Daigle, Kwok, & Mackie, 2008).

4.3 | Slowed arrestin translocation produces potentiated signalling

This study also contributes to the understanding of the role of arrestin translocation kinetics on G protein activity, which is shown to be as important as the extent of arrestin translocation. The *pxxxp* motif (D1; S425A/S429A) has been extensively studied *in vitro* and *in vivo*. The original study describing this mutant suggested that the S425/S429 sites were important for desensitisation, but not internalisation of the receptor, designating this mutant 'desensitisation deficient' (Jin et al., 1999). A subsequent study on this mutant identified via immunocytochemistry that it could interact with arrestin-3 with a time course similar to wild type CB_1 receptor and had a slightly

reduced internalisation capacity (Daigle, Kearn, & Mackie, 2008). The real-time arrestin-BRET data in this study identified changes in kinetics that were not observed in the original study, which may be due to differences in the assays employed by different studies to quantify arrestin-CB_1 receptor interaction (Daigle, Kearn, & Mackie, 2008). In fact, this mutant had equivalent arrestin-2/3 translocation steady state as the wild type receptor, but a slowed translocation rate, which manifested as potentiated peak G protein dissociation, but was still desensitisation-competent. This mutant has been demonstrated *in vivo* to confer cannabinoid hypersensitivity and delayed/reduced development of tolerance in mice, consistent with the reduced signal regulation described here (Morgan et al., 2014; Nealon et al., 2019). This is also congruent with the *in vivo* cannabinoid pharmacology of arrestin-3 knockout mice (Breivogel et al., 2008, 2013).

We did not observe enhanced arrestin-2 interaction with the S245A/S429A CB_1 receptor mutant, which has previously been reported (Delgado-Peraza et al., 2016). The former study (Delgado-Peraza et al., 2016) observes potentiated pERK signalling for S425A/S429A, which is congruent with another (Daigle, Kearn, & Mackie, 2008), however the two studies attribute this increased signalling to either enhanced arrestin-2 interaction or reduced desensitisation, respectively. The data presented here support the hypothesis that the potentiated pERK signalling of the S425A/S429A mutant is likely a result of enhanced G protein activity, due to slowed interaction with both arrestin subtypes, supporting the original suggestion (Daigle, Kearn, & Mackie, 2008).

4.4 | Proximal and distal sites are independently important for arrestin translocation

The observation that mutation of proximal, but not distal C-terminal phosphorylation sites reduces the rate of translocation suggests that these two proximal sites (S425, S429) may act as initial contact points between CB_1 receptor and arrestin, stabilising arrestin to fully engage with the distal C-terminus of CB_1 receptor. Previous studies have suggested that arrestin-GPCR binding may occur in two different modes, 'hanging' or 'full engagement' characterised by strength of the binding, with the hanging conformation possibly an intermediate binding state (Asher et al., 2022; Park et al., 2016; Shukla et al., 2014). These two conformations have been suggested to be functionally distinct and each may be stabilised by different ligands (Kawakami et al., 2022). The observation that two distinct parts of the C-terminus of CB_1 receptor may be involved in different parts of arrestin binding hints towards a molecular basis for different arrestin binding conformations. Analogous observations have been made for the **μ-opioid receptor**, where proximal and distal serine/threonine clusters in the C-terminus have been demonstrated to be independently important for arrestin translocation (Lau et al., 2011; Miess et al., 2018; Yousuf et al., 2015). Whilst the methods employed in this study cannot distinguish between hanging or full engagement arrestin conformations for CB_1 receptor, the role of S425/S429 in these different arrestin-binding modes should be investigated in future.

This study has identified how different serine/threonine phosphorylation sites within the CB_1 receptor C-terminus affect arrestin-2 and arrestin-3 translocation in response to a high-efficacy ligand. Arrestin translocation to CB_1 receptor does not entirely depend on *pxxp* motifs and progressive total phosphorylation of the C-terminus appears proportional to efficacy of arrestin translocation, rather than a particular pattern. Both arrestin subtypes require the same phosphorylation patterns to interact with CB_1 receptor, which is an important consideration for arrestin subtype bias. Two different phosphorylation clusters in the CB_1 receptor C-terminus are independently important for translocation and may be responsible for different arrestin binding conformations. Together, these data have considerable implications for the premise and development of drugs which attempt to drive subtype-selective interactions between arrestins and CB_1 receptor via unique phosphorylation patterns.

ACKNOWLEDGEMENTS

The authors would like to acknowledge Dr Rob Woolley from the Otago Micro and Nanoscale Imaging (OMNI) facility for image acquisition and analysis assistance. Open access publishing facilitated by University of Otago, as part of the Wiley - University of Otago agreement via the Council of Australian University Librarians.

CONFLICT OF INTEREST

The authors declare no conflicts of interest.

AUTHOR CONTRIBUTIONS

Jamie J. Manning designed and performed experiments, analysed the data and wrote the manuscript. Gabriel Rawcliffe assisted with design and generation of receptor mutants. David B. Finlay and Michelle Glass oversaw all aspects of the project.

DECLARATION OF TRANSPARENCY AND SCIENTIFIC RIGOUR

This Declaration acknowledges that this paper adheres to the principles for transparent reporting and scientific rigour of preclinical research as stated in the *BJP* guidelines for Design & Analysis and Immunoblotting and Immunochemistry, and as recommended by funding agencies, publishers, and other organisations engaged with supporting research.

DATA AVAILABILITY STATEMENT

The data that support the findings of this study are available from the corresponding author upon reasonable request.

ORCID

Jamie J. Manning https://orcid.org/0000-0002-6945-2254
Gabriel Rawcliffe https://orcid.org/0000-0003-4157-9680
David B. Finlay https://orcid.org/0000-0002-3160-2931
Michelle Glass https://orcid.org/0000-0002-5997-6898

REFERENCES

Alexander, S. P., Christopoulos, A., Davenport, A. P., Kelly, E., Mathie, A., Peters, J. A., Veale, E. L., Armstrong, J. F., Faccenda, E., Harding, S. D., Pawson, A. J., Southan, C., Davies, J. A., Abbracchio, M. P., Alexander, W., Al-hosaini, K., Bäck, M., Barnes, N. M., Bathgate, R., … Ye, R. D. (2021). THE CONCISE GUIDE TO PHARMACOLOGY 2021/22: G protein-coupled receptors. *British Journal of Pharmacology*, *178*(S1), S27–S156. https://doi.org/10.1111/bph.15538

Alexander, S. P. H., Roberts, R. E., Broughton, B. R. S., Sobey, C. G., George, C. H., Stanford, S. C., Cirino, G., Docherty, J. R., Giembycz, M. A., Hoyer, D., & Ahluwalia, A. (2018). Goals and practicalities of immunoblotting and immunohistochemistry: A guide for submission to the *British Journal of Pharmacology*. *British Journal of Pharmacology*, *175*, 407–411. https://doi.org/10.1111/bph.14112

Asher, W. B., Terry, D. S., Gregorio, G. G. A., Kahsai, A. W., Borgia, A., Xie, B., Modak, A., Zhu, Y., Jang, W., Govindaraju, A., Huang, L. Y., Inoue, A., Lambert, N. A., Gurevich, V. V., Shi, L., Lefkowitz, R. J., Blanchard, S. C., & Javitch, J. A. (2022). GPCR-mediated β-arrestin activation deconvoluted with single-molecule precision. *Cell*, *185*(10), 1661–1675e16. https://doi.org/10.1016/J.CELL.2022.03.042

Banister, S. D., Longworth, M., Kevin, R., Sachdev, S., Santiago, M., Stuart, J., Mack, J. B. C., Glass, M., Mcgregor, I. S., Connor, M., & Kassiou, M. (2016). Pharmacology of Valinate and tert-Leucinate synthetic cannabinoids 5F-AMBICA, 5F-AMB, 5F-ADB, AMB-FUBINACA, MDMB-FUBINACA, MDMB-CHMICA, and their analogues. *ACS Chemical Neuroscience*, *7*(9), 1241–1524. https://doi.org/10.1021/acschemneuro.6b00137

Breivogel, C. S., Lambert, J. M., Gerfin, S., Huffman, J. W., & Razdan, R. K. (2008). Sensitivity to Δ9-tetrahydrocannabinol is selectively enhanced in beta-arrestin2−/− mice. *Behavioural Pharmacology*, *19*(4), 298–307. https://doi.org/10.1097/FBP.0b013e328308f1e6

Breivogel, C. S., Puri, V., Lambert, J. M., Hill, D. K., Huffman, J. W., & Razdan, R. K. (2013). The influence of beta-arrestin2 on cannabinoid CB1 receptor coupling to G-proteins and subcellular localization and relative levels of beta-arrestin1 and 2 in mouse brain. *Journal of Receptors and Signal Transduction*, *33*(6), 367–379. https://doi.org/10.3109/10799893.2013.838787

Curtis, M. J., Alexander, S. P. H., Cirino, G., George, C. H., Kendall, D. A., Insel, P. A., Izzo, A. A., Ji, Y., Panettieri, R. A., Patel, H. H., Sobey, C. G., Stanford, S. C., Stanley, P., Stefanska, B., Stephens, G. J., Teixeira, M. M., Vergnolle, N., & Ahluwalia, A. (2022). Planning experiments: Updated guidance on experimental design and analysis and their reporting III. *British Journal of Pharmacology*, *179*(15), 3907–3913. https://doi.org/10.1111/bph.15868

Daigle, T. L., Kearn, C. S., & Mackie, K. (2008). Rapid CB1 cannabinoid receptor desensitization defines the time course of ERK1/2 MAP kinase signaling. *Neuropharmacology*, *54*(1), 36–44. https://doi.org/10.1016/j.neuropharm.2007.06.005

Daigle, T. L., Kwok, M. L., & Mackie, K. (2008). Regulation of CB1 cannabinoid receptor internalization by a promiscuous phosphorylation-dependent mechanism. *Journal of Neurochemistry*, *106*(1), 70–82. https://doi.org/10.1111/j.1471-4159.2008.05336.x

Delgado-Peraza, F., Ahn, K. H., Nogueras-Ortiz, C., Mungrue, I. N., Mackie, K., Kendall, D. A., & Yudowski, G. A. (2016). Mechanisms of biased β-arrestin-mediated signaling downstream from the cannabinoid 1 receptor. *Molecular Pharmacology*, *89*(6), 618–629. https://doi.org/10.1124/mol.115.103176

Donthamsetti, P., Quejada, J. R., Javitch, J. A., Gurevich, V. V., & Lambert, N. A. (2015). Using bioluminescence resonance energy transfer (BRET) to characterize agonist-induced Arrestin recruitment to modified and unmodified G protein-coupled receptors. *Current Protocols in Pharmacology*, *70*(1), 2–14. https://doi.org/10.1002/0471141755.ph0214s70

Finlay, D. B., Cawston, E. E., Grimsey, N. L., Hunter, M. R., Korde, A., Vemuri, V. K., Makriyannis, A., & Glass, M. (2017). Gαs signalling of the CB1 receptor and the influence of receptor number. *British Journal of Pharmacology*, *174*(15), 2545–2562. https://doi.org/10.1111/bph.13866

Finlay, D. B., Joseph, W. R., Grimsey, N. L., & Glass, M. (2016). GPR18 undergoes a high degree of constitutive trafficking but is unresponsive to N-Arachidonoyl glycine. *PeerJ*, *4*, e1835. https://doi.org/10.7717/peerj.1835

Finlay, D. B., Manning, J. J., Ibsen, M. S., Macdonald, C. E., Patel, M., Javitch, J. A., Banister, S. D., & Glass, M. (2019). Do toxic synthetic cannabinoid receptor agonists have signature in vitro activity profiles? A case study of AMB-FUBINACA. *ACS Chemical Neuroscience*, *10*(10), 4350–4360. https://doi.org/10.1021/acschemneuro.9b00429

Gamage, T. F., Farquhar, C. E., Lefever, T. W., Marusich, J. A., Kevin, R. C., McGregor, I. S., Wiley, J. L., & Thomas, B. F. (2018). Molecular and behavioral pharmacological characterization of abused synthetic cannabinoids MMB- and MDMB-FUBINACA, MN-18, NNEI, CUMYL-PICA, and 5-Fluoro-CUMYL-PICA. *Journal of Pharmacology and Experimental Therapeutics*, *365*(2), 437–446. https://doi.org/10.1124/JPET.117.246983

Grimsey, N. L., Narayan, P. J., Dragunow, M., & Glass, M. (2008). A novel high-throughput assay for the quantitative assessment of receptor trafficking. *Clinical and Experimental Pharmacology and Physiology*, *35*(11), 1377–1382. https://doi.org/10.1111/j.1440-1681.2008.04991.x

Hoare, S. R. J., Tewson, P. H., Quinn, A. M., Hughes, T. E., & Bridge, L. J. (2020). Analyzing kinetic signaling data for G-protein-coupled receptors. *Scientific Reports*, *10*(1), 1, 12263–23. https://doi.org/10.1038/s41598-020-67844-3

Hoare, S. R. J., Tewson, P. H., Sachdev, S., Connor, M., Hughes, T. E., & Quinn, A. M. (2022). Quantifying the kinetics of signaling and Arrestin recruitment by nervous system G-protein coupled receptors. *Frontiers in Cellular Neuroscience*, *15*, 558. https://doi.org/10.3389/fncel.2021.814547

Hsieh, C., Brown, S., Derleth, C., & Mackie, K. (1999). Internalization and recycling of the CB1 cannabinoid receptor. *Journal of Neurochemistry*, *73*(2), 493–501. https://doi.org/10.1046/j.1471-4159.1999.0730493.x

Ibsen, M. S., Finlay, D. B., Patel, M., Javitch, J. A., Glass, M., & Grimsey, N. L. (2019). Cannabinoid CB1 and CB2 receptor-mediated Arrestin translocation: Species, subtype, and agonist-dependence. *Frontiers in Pharmacology*, *10*, 350. https://doi.org/10.3389/fphar.2019.00350

Jin, W., Brown, S., Roche, J. P., Hsieh, C., Celver, J. P., Kovoor, A., Chavkin, C., & Mackie, K. (1999). Distinct domains of the CB1 cannabinoid receptor mediate desensitization and internalization. *The Journal of Neuroscience*, *19*(10), 3773–3780. https://doi.org/10.1523/JNEUROSCI.19-10-03773.1999

Kawakami, K., Yanagawa, M., Hiratsuka, S., Yoshida, M., Ono, Y., Hiroshima, M., Ueda, M., Aoki, J., Sako, Y., & Inoue, A. (2022). Heterotrimeric Gq proteins act as a switch for GRK5/6 selectivity underlying β-arrestin transducer bias. *Nature Communications*, *13*(1), 1–16. https://doi.org/10.1038/s41467-022-28056-7

Komolov, K. E., & Benovic, J. L. (2018). G protein-coupled receptor kinases: Past, present and future. *Cellular Signalling*, *41*, 17–24. https://doi.org/10.1016/j.cellsig.2017.07.004

Krishna Kumar, K., Shalev-Benami, M., Robertson, M. J., Hu, H., Banister, S. D., Hollingsworth, S. A., Latorraca, N. R., Kato, H. E., Hilger, D., Maeda, S., Weis, W. I., Farrens, D. L., Dror, R. O., Malhotra, S. V., Kobilka, B. K., & Skiniotis, G. (2019). Structure of a signaling cannabinoid receptor 1-G protein complex. *Cell*, *176*(3), 409–411. https://doi.org/10.1016/J.CELL.2018.11.040

Lau, E. K., Trester-Zedlitz, M., Trinidad, J. C., Kotowski, S. J., Krutchinsky, A. N., Burlingame, A. L., & Von Zastrow, M. (2011). Quantitative encoding of the effect of a partial agonist on individual opioid receptors by multisite phosphorylation and threshold detection. *Science Signaling*, *4*(185), ra52–ra52. https://doi.org/10.1126/scisignal.2001748

Manning, J. J., Green, H. M., Glass, M., & Finlay, D. B. (2021). Pharmacological selection of cannabinoid receptor effectors: Signalling, allosteric modulation and bias. *Neuropharmacology*, *193*, 108611. https://doi.org/10.1016/j.neuropharm.2021.108611

Matti, C., Salnikov, A., Artinger, M., D'Agostino, G., Kindinger, I., Uguccioni, M., Thelen, M., & Legler, D. F. (2020). ACKR4 recruits GRK3 prior to β-arrestins but can scavenge chemokines in the absence of β-Arrestins. *Frontiers in Immunology*, *11*, 720. https://doi.org/10.3389/fimmu.2020.00720

Mayer, D., Damberger, F. F., Samarasimhareddy, M., Feldmueller, M., Vuckovic, Z., Flock, T., Bauer, B., Mutt, E., Zosel, F., Allain, F. H. T., Standfuss, J., Schertler, G. F. X., Deupi, X., Sommer, M. E., Hurevich, M., Friedler, A., & Veprintsev, D. B. (2019). Distinct G protein-coupled receptor phosphorylation motifs modulate arrestin affinity and activation and global conformation. *Nature Communications*, *10*(1), 1, 1261–14. https://doi.org/10.1038/s41467-019-09204-y

Miess, E., Gondin, A. B., Yousuf, A., Steinborn, R., Mösslein, N., Yang, Y., Göldner, M., Ruland, J. G., Bünemann, M., Krasel, C., Christie, M. J., Halls, M. L., Schulz, S., & Canals, M. (2018). Multisite phosphorylation is required for sustained interaction with GRKs and arrestins during rapid -opioid receptor desensitization. *Science Signaling*, *11*(539), eaas9609. https://doi.org/10.1126/scisignal.aas9609

Morgan, D. J., Davis, B. J., Kearn, C. S., Marcus, D., Cook, A. J., Wager-Miller, J., Straiker, A., Myoga, M. H., Karduck, J., Leishman, E., Sim-Selley, L. J., Czyzyk, T. A., Bradshaw, H. B., Selley, D. E., & Mackie, K. (2014). Mutation of putative GRK phosphorylation sites in the cannabinoid receptor 1 (CB1R) confers resistance to cannabinoid tolerance and hypersensitivity to cannabinoids in mice. *The Journal of Neuroscience: The Official Journal of the Society for Neuroscience*, *34*(15), 5152–5163. https://doi.org/10.1523/JNEUROSCI.3445-12.2014

Nealon, C. M., Henderson-Redmond, A. N., Hale, D. E., & Morgan, D. J. (2019). Tolerance to WIN55,212-2 is delayed in desensitization-resistant S426A/S430A mice. *Neuropharmacology*, *148*, 151–159. https://doi.org/10.1016/j.neuropharm.2018.12.026

Pacher, P., Bátkai, S., & Kunos, G. (2006). The endocannabinoid system as an emerging target of pharmacotherapy. *Pharmacological Reviews*, *58*(3), 389–462. https://doi.org/10.1124/pr.58.3.2

Park, J. Y., Lee, S. Y., Kim, H. R., Seo, M. D., & Chung, K. Y. (2016). Structural mechanism of GPCR-arrestin interaction: Recent breakthroughs. *Archives of Pharmacal Research*, *39*(3), 293–301. https://doi.org/10.1007/s12272-016-0712-1

Patel, M., Manning, J. J., Finlay, D. B., Javitch, J. A., Banister, S. D., Grimsey, N. L., & Glass, M. (2020). Signalling profiles of a structurally diverse panel of synthetic cannabinoid receptor agonists. *Biochemical Pharmacology*, *175*, 113871. https://doi.org/10.1016/j.bcp.2020.113871

Patel, M., Matti, C., Grimsey, N. L., Legler, D. F., Javitch, J. A., Finlay, D. B., & Glass, M. (2022). Delineating the interactions between the cannabinoid CB2 receptor and its regulatory effectors; β-arrestins and GPCR kinases. *British Journal of Pharmacology*, *179*(10), 2223–2239. https://doi.org/10.1111/bph.15748

Sachdev, S., Vemuri, K., Banister, S. D., Longworth, M., Kassiou, M., Santiago, M., Makriyannis, A., & Connor, M. (2019). In vitro determination of the efficacy of illicit synthetic cannabinoids at CB1 receptors. *British Journal of Pharmacology*, *176*(24), 4653–4665. https://doi.org/10.1111/bph.14829

Shukla, A. K., Westfield, G. H., Xiao, K., Reis, R. I., Huang, L. Y., Tripathi-Shukla, P., Qian, J., Li, S., Blanc, A., Oleskie, A. N., Dosey, A. M., Su, M., Liang, C. R., Gu, L. L., Shan, J. M., Chen, X., Hanna, R., Choi, M., Yao, X. J., … Lefkowitz, R. J. (2014). Visualization of arrestin recruitment by a G-protein-coupled receptor. *Nature*, *512*(7513), 218–222. https://doi.org/10.1038/nature13430

Straiker, A., Wager-Miller, J., & Mackie, K. (2012). The CB1 cannabinoid receptor C-terminus regulates receptor desensitization in autaptic hippocampal neurones. *British Journal of Pharmacology*, *165*(8), 2652–2659. https://doi.org/10.1111/j.1476-5381.2011.01743.x

Wootten, D., Christopoulos, A., Marti-Solano, M., Babu, M. M., & Sexton, P. M. (2018). Mechanisms of signalling and biased agonism in G protein-coupled receptors. *Nature Reviews Molecular Cell Biology*, *19*(10), 638–653. https://doi.org/10.1038/s41580-018-0049-3

Yousuf, A., Miess, E., Sianati, S., Du, Y. P., Schulz, S., & Christie, M. J. (2015). Role of phosphorylation sites in desensitization of μ-opioid receptor. *Molecular Pharmacology*, *88*(4), 825–835. https://doi.org/10.1124/MOL.115.098244

How to cite this article: Manning, J. J., Rawcliffe, G., Finlay, D. B., & Glass, M. (2023). Cannabinoid 1 (CB_1) receptor arrestin subtype-selectivity and phosphorylation dependence. *British Journal of Pharmacology*, *180*(3), 369–382. https://doi.org/10.1111/bph.15973